

Study on the influence of pipe diameter and burial depth on the variation of magnetic field of oil pipeline

Ruonan Zhou, Hao Chen

School of Southwest Petroleum University, Chengdu 610000, China

Abstract

In this paper, the stress concentration phenomenon in the overhanging pipe section of buried oil and gas transmission pipeline is investigated by using ANSYS finite element analysis software to study the stress and magnetic field distribution state of the pipeline at different pipe diameters and different burial depths, and the variation relationship of magnetic memory signal in the overhanging pipe section of oil and gas transmission pipeline is analyzed to provide theoretical pavement for the engineering application of magnetic memory detection technology. With the end point of the research pipeline as a fixed constraint, the analytical model of the oil and gas transmission pipeline is established under the condition of small deformation of the oil and gas transmission pipeline, and the stress and magnetic field intensity changes of five different pipe diameters are explored separately by using ANSYS finite element analysis software. According to the deformation displacement distribution diagram, the relationship between stress and magnetic field strength changes, etc., it can be concluded that the displacement of the overhanging pipe section decreases non-linearly as the pipe diameter increases sequentially. The magnetic field strength decreases when the pipe diameter increases gradually. With the sequential increase of burial depth, the displacement change of the overhanging pipe section is close to a linear decrease. As the burial depth increases, the stress in the study unit gradually increases, and the magnetic field strength increases with the increase of the burial depth.

Keywords

Magnetic memory; Finite element; Oil and gas pipelines.

1. Introduction

In recent years, with the development of China's "West-East Gas Transmission" project, buried pipelines have become the main way to transport oil and gas, an important channel to transport the rich real estate resources in the west to the eastern development areas, bringing the foundation of social development for coastal people. Oil and gas is the first step in the development of today's society, and its demand has been continuously growing without seeing a decline. The development of the eastern coastal region cannot be achieved without oil and gas. Buried pipeline as the transmission carrier of oil and gas, from the west to the east to experience the topographic changes, there are also human plowing, road conditions, river scouring, flash floods and other acts of influence, so that buried pipeline in operation is very easy to form overhanging pipe section, to the detriment of safety, bringing serious losses to the country.

In order to explore the influence of pipe diameter on the overhanging pipe section, this paper uses metal magnetic memory detection technology to get the displacement change distribution area of the overhanging pipe section by establishing the mechanical model of the overhanging pipe section with different pipe diameters, extracting the stress from the mechanical model, calculating the magnetic permeability from the stress in the existing force-magnetic model, finding out the change law of the material permeability, analyzing the relationship between

magnetic permeability and magnetic field and the development trend, and providing the Theoretical pavement for the development of metal magnetic memory detection technology.

Metal magnetic memory detection technology started at the end of the last century. Professor Doubov [1] has been working in the field of metal magnetic memory detection technology and has made a significant contribution to its development, not only in theoretical aspects, but also in the development of the corresponding magnetic memory detection instruments in order to increase the practicality of the technology. The advent of the magnetic memory testing instrument has facilitated the development of the technique and made it easier than ever to study.

Maciej Roskosz [2] of the University of Silesia used the metal magnetic memory inspection technique to inspect and evaluate welded joints, comparing the results of the magnetic memory inspection technique with those of radiological inspection. The metal magnetic memory detection technique allows the detection of defects at the microscopic level in welded joints during the production stage, which concentrate the stresses from the working load.

Mahdi Moonesan [3] et al. investigated the role of the residual magnetic field on the intensity of stress-influenced magnetization by placing mild steel samples in different initial magnetic fields and collecting the corresponding magnetic signals, pointing out a strong correlation between the residual magnetic field and its corresponding stress-influenced magnetic field, with the magnetic field intensity of the specimen decreasing as the initial residual field increases.

In addition to Mahdi Moonesan, Wilson et al [4] also studied the stresses obtained by introducing a residual magnetic field for complex specimens based on the metal magnetic memory detection technique and analyzed the magnetic field form and the rate of change, concluding that the technique has a critical role.

Kaleta Jerzy et al [5] designed a system for measuring the strength of the magnetic field around a ferromagnetic specimen under cyclic (or static) loading and developed a new camera for monitoring the magnetogram of the sample. The measurement principle of the system is based on the inverse magnetostriction effect. Assuming that there is no applied magnetic field and that the whole effect is entirely due to cyclic mechanical loading, it was concluded that the measurement device is best suited for checking the plane stress situation.

Koson Schab et al [6] carried out health monitoring of crane structures by magnetic memory detection techniques and found that the magnetic field strength is very sensitive to changes in dynamic loads, mechanism movements and transient operations of the drive system and that disturbances caused by operational changes can be easily identified and the disturbances are easily removed from the diagnostic signal.

At present, metal magnetic memory detection technology has been recognized by most countries, such as China, the United States, the United Kingdom, Australia, Russia and other countries, this method provides practical and reasonable detection methods as well as accurate results when people study non-contact problems and fine structure problems.

2. Mechanical analysis of buried suspended pipe section

2.1. Force situation

Buried oil and gas transmission pipelines are buried in the soil for a long time and suffer from disasters such as rainwater washout and earthquakes, forming suspended pipe sections inside the soil. The creation of buried suspended pipe section changes the original force condition of the pipeline. As the original soil is lost by rain, the position of some rocks in the soil is changed, and the buried suspended pipe section will be deformed under the action of its own gravity and

internal medium pressure, so that the stress distribution around the long-distance pipeline is changed.

The two ends of the suspended pipe section are buried in the soil, and after the force changes, the two ends of the suspended pipe section will also sink. Then, the suspended pipe section is not only subjected to its own gravity, internal pressure, but also to the reverse force of the soil on the pipe. The analytical model is an elastic foundation beam, taking the point of zero elastic deformation in the soil as a fixed point. The displacement change of the part of the pipe in contact with the soil is approximately linear in practical engineering, so the action of the soil on the suspended pipe section can be replaced by a spring of the same distance, increasing the force of the soil on the pipe and the axial force of the pipe. This method is more in line with the actual force situation of buried suspended pipe sections.

2.2. Model and boundary conditions

In view of the complex contact action of soil and pipe and the complicated cohesion of soil, soil and pipe friction, in order to facilitate analysis and calculation, the following assumptions are made in this paper.

(1) Assuming that the soil is hard, the end point of the buried soil of the suspended pipe section selected for the study is treated as a fixed end, the influence of the soil on the buried end of the suspended pipe section is treated as a uniform distribution, and the whole pipe becomes continuous.

(2) The unit type of the buried suspended pipe section is defined as Beam189 beam unit, and the simulated suspended pipe section is laid horizontally without slope and other considerations, and no pinch angle exists.

(3) The force and deformation of the suspended pipe section are assumed to be symmetrically distributed along the axial direction.

(4) The surface of the suspended pipe section is free of any defects.

(5) The overhanging pipe section of the oil and gas transmission pipeline is exposed to the air.

(6) The effects of temperature stress and residual welding stress are not considered.

(7) The variation of the geomagnetic field is neglected and is a fixed value.

Beam189 beam cells are used to model buried overhanging pipe sections. Beam189 beam cells are suitable for beam structures with large thicknesses but short volumes, and Beam189 beam cells have a variety of cross sections. The model of Timuchenko's beam theory takes into account shear stress and rotational inertia, and is therefore an excellent and outstanding theory that fits the actual situation.

In Beam189 beam cell, each node has at least six degrees of freedom [28], i.e., translation and rotation in x, y and z directions and around three axes. In some cases, there is an additional warpage at each node, but in many literatures, the warpage is not considered directly or the result of warpage is neglected.

After Beam189 beam unit is selected, the properties of the suspended pipe section, such as the tensile modulus, transverse deformation coefficient and material density, are set. In this paper, for the buried suspended pipe section, after reading several studies, the material selected for the study is Q235, with a tensile modulus of 210 GPa, a transverse deformation coefficient of 0.3, and a pipe density ρ of 7850 kg/m³. The soil around the suspended pipe section is taken into account the presence of stones and the influence of ground motion on the soil, so the soil density ρ_s is taken as 2500 kg/m³.

However, in this paper, we assume that the end point of the oil and gas pipeline buried in the soil is a fixed constraint and the influence of the soil on the buried end of the suspended pipe section is treated as a uniformly distributed load, and the load of the whole pipeline is continuous.

When Beam189 beam cell is used to construct the model, Δx , Δy and Δz are the displacements in x, y and z directions respectively, and the degrees of freedom of Δx , Δy and Δz are constrained in all three directions at the end point of the suspended pipe section buried in the soil. To simplify the effect of fluid inside the oil and gas transmission pipeline on the pipeline, the internal pressure of the pipeline is equated to a uniform load, which is applied to the beam unit. In this paper, the suspension length and the selected length of the pipe buried in the soil remain unchanged, and the material parameters of the oil and gas transmission pipeline are not changed, and only the effect of the change of pipe diameter and burial depth on the magnetic memory signal is studied. In this paper, the length of the suspended pipe section is taken as 50 m. When dividing the cells, Mesh Attributes is used to specify the directional points, and after that, it is divided along the axial direction of the pipe.

The magnetic memory study involves a comprehensive analysis of the coupled fields, i.e., the force and magnetic fields are combined and analyzed to derive the coupling results under the joint action of the force and magnetic fields.

3. Finite element model

3.1. Mechanical model for different pipe diameters

In this paper, the stress variations for different pipe diameters are first considered. The modeling was performed using ANSYS Mechanical APDL 19.0 software. The cross-sections of the five beam unit models are shown in Figure1-Figure 5, respectively.

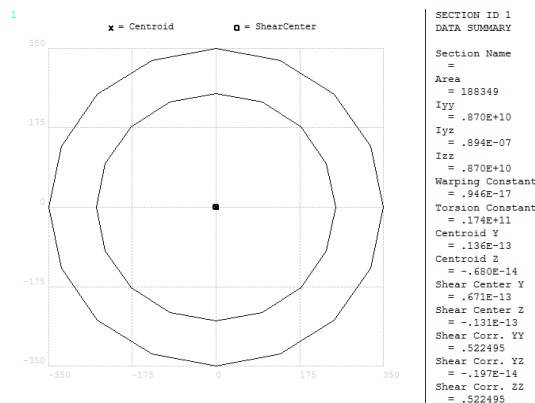


Fig.1 600mm pipe section data

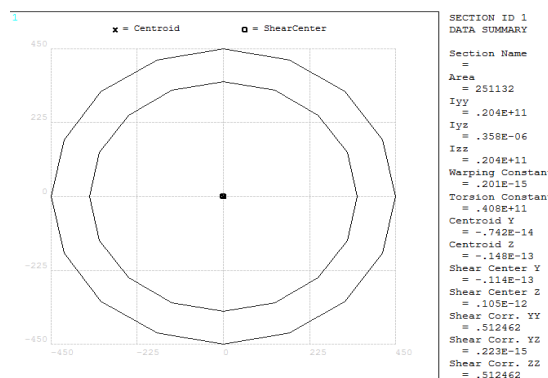


Fig.2 700mm pipe section data

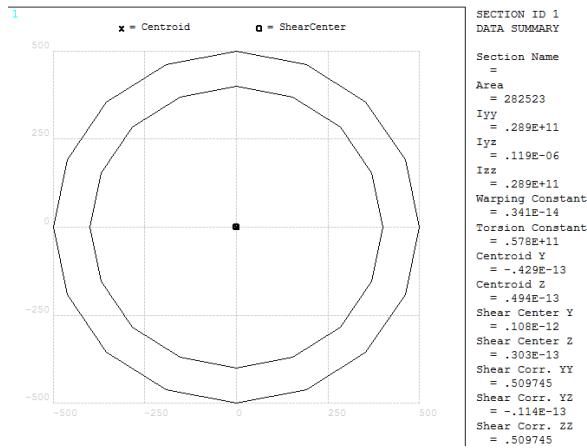


Fig.3 800mm pipe section data

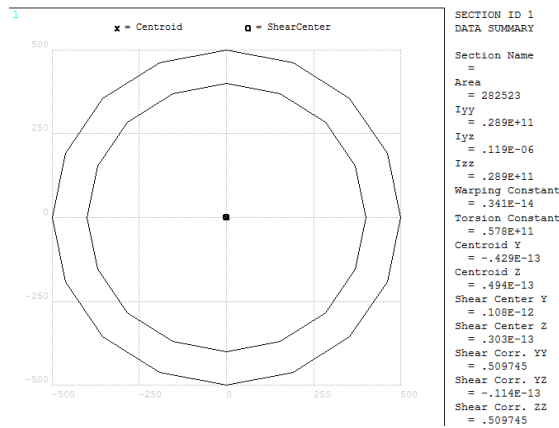


Fig.4 900mm pipe section data

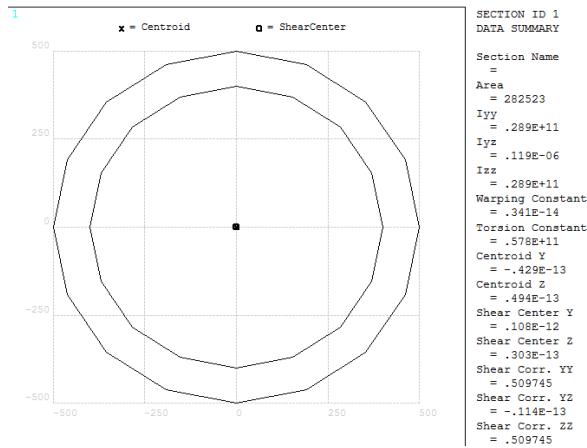


Fig.5 1000mm pipe section data

3



Fig.6 Geometric modeling

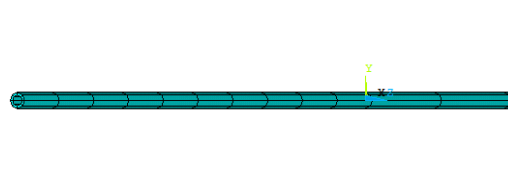


Fig.7 Grid division results

4. Results of magnetic analysis of mechanical forces

The displacement diagrams of five different pipe diameters of oil and gas transmission pipeline models are shown in Figure1 - Figure.6

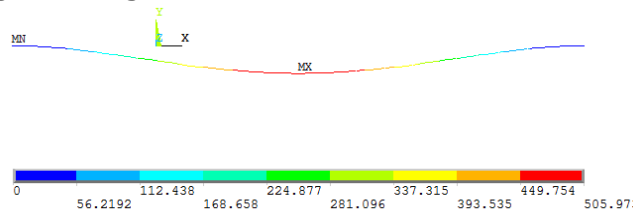


Fig.1 Deformation displacement diagram of pipe with 600mm outer diameter

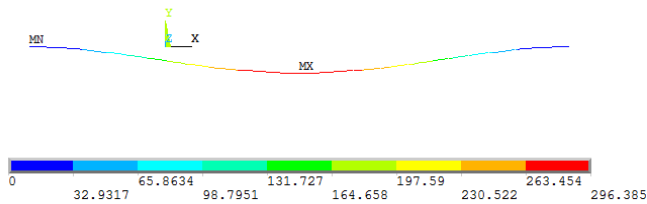


Fig.2 Deformation displacement diagram of pipe with 700mm outer diameter

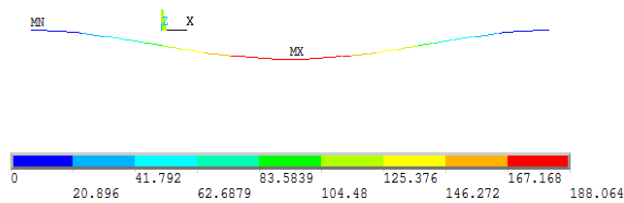


Fig.3 Deformation displacement diagram of pipe with 800mm outer diameter

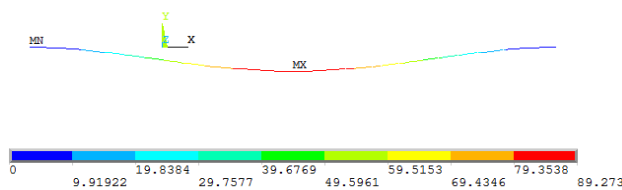


Fig.4 Deformation displacement diagram of pipe with 900mm outer diameter

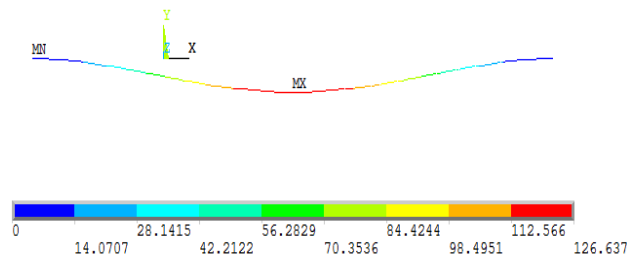


Fig.5 Deformation displacement diagram of pipe with 1000mm outer diameter

The displacement variation and magnetic field strength comparison folding diagrams for five different pipe diameters of oil and gas transmission pipelines are shown in Fig.6 Fig.7.

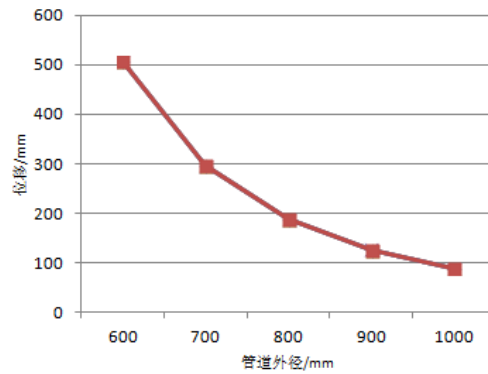


Fig.6 Variation of displacement of suspended pipe section with pipe diameter

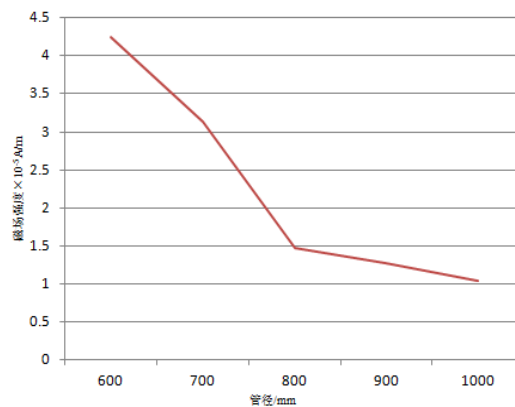


Fig.7 Variation of magnetic field strength with pipe diameter for suspended pipe section

5. Mechanical models for different burial depths

After obtaining the laws of pipe diameter and displacement and stress for the suspended pipe sections of five pipe diameters of oil and gas transmission pipelines, the stress variation at different burial depths was next explored.

The variation in burial depth causes the soil forces on the pipe at both ends of the pipe to change as well. Q235 pipes with an external diameter of 1000 mm were used to study the stress variation at different burial depths.

The initial stress is generated and applied, and the initial stress file of the model with 1000mm outer diameter can be reused to avoid the operation steps of generating the initial stress file and applying the initial stress repeatedly twice, and also to save time. The operation parameters such as cell type, section setting, model establishment, attribute assignment, mesh division and partial load application are the same when the burial depth is changed.

5.1. Force Magnetic Analysis

The trends of displacement and stress were obtained for different pipe diameters and different burial depths, so then the magnetic permeability was analyzed. The overhanging pipe section is deformed, then its stress distribution is changed accordingly. After obtaining the stresses, the maximum stresses are calculated according to the following simple relations (1) and (5). BENDING STRESS represents the bending stress, SBYT and SBYB both represent the Y-side bending stress, SMAX represents the maximum stress, and SDIR represents the axial stress.

$$\text{BENDING STRESS} = 1/2(\text{SBYT} + \text{SBYB}) \tag{1}$$

$$\text{SMAX} = \text{SDIR} + \text{BENDING STRESS} \tag{2}$$

The relative magnetic permeability of the material is calculated according to Equation (3)

$$\mu_\sigma = \frac{B_m^2 + \sqrt{B_m^4 - 8\sigma\lambda_m\mu_0\mu_1 B_m^2}}{4\sigma\lambda_m\mu_0} \tag{3}$$

Equation (3) is calculated in the relative permeability, due to the need to use the absolute permeability in Equation (5), so first use Equation (4) to calculate the absolute permeability.

$$\mu_\sigma = \frac{\mu}{\mu_0} \tag{4}$$

The absolute magnetic permeability calculated by Equation (4) is brought into Equation(5). The magnetic induction strength in Chengdu area is 4.41×10^{-5} T. So the magnetic field strength of the suspended pipe section can be calculated by Equation(5).

$$H = \frac{B}{\mu} \tag{5}$$

5.2. Mechanical force magnetic analysis results

The displacement diagrams for five different pipe diameters of oil and gas transmission pipeline models are shown in Figure 1 - Figure 5.

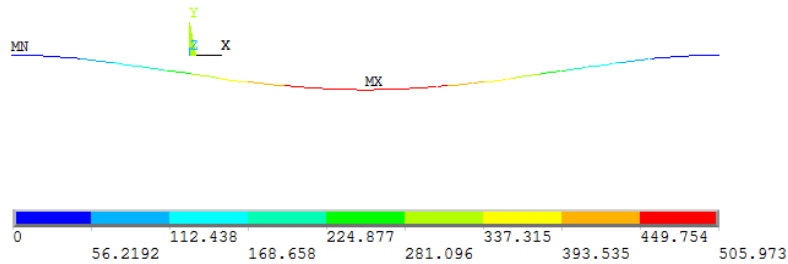


Fig.1 Deformation displacement diagram of pipe with 600mm outer diameter

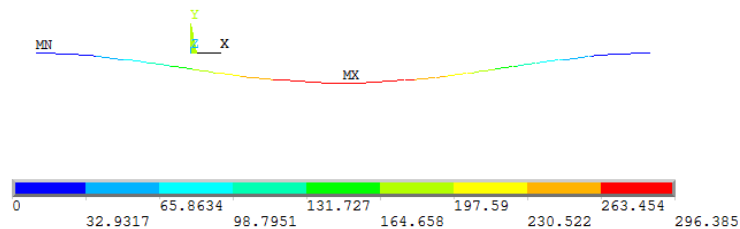


Fig.2 Deformation displacement diagram of pipe with 700mm outer diameter

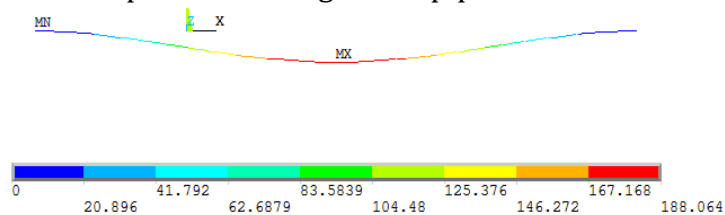


Fig.3 Deformation displacement diagram of pipe with 800mm outer diameter

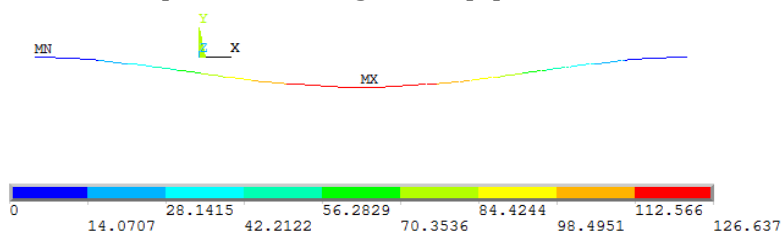


Fig.4 Deformation displacement diagram of pipe with 900mm outer diameter

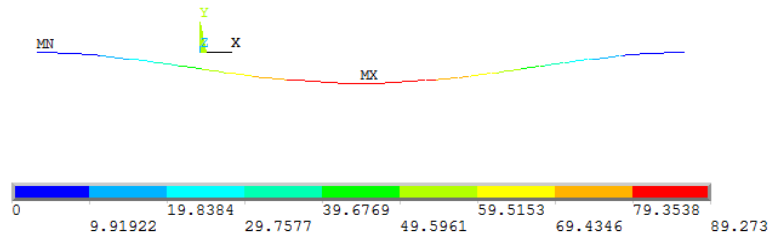


Fig.5 Deformation displacement diagram of pipe with 1000mm outer diameter
The values of displacement, bending stress, and axial stress for five different pipe diameter models are shown in Table1.

Table 1 Values of displacement, bending stress and axial stress when the pipe diameter changes

Pipe outside diameter/m	Displacement/mm	Axial stress/MPa	Y-side bending stress /MPa	Y-side bending stress/MPa
600	505.973	0.339	0.386	0.147
700	296.385	0.178	0.354	0.171
800	188.064	0.067	0.176	0.108
900	126.637	0.103	0.058	0.096
1000	89.273	0.084	0.049	0.081

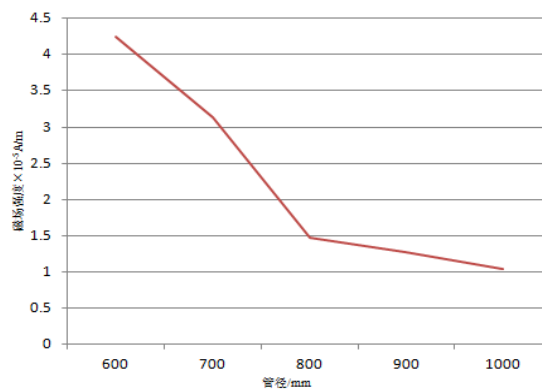


Fig.6 Variation of magnetic field strength with pipe diameter in the overhanging pipe section
The displacement distribution of five oil and gas transmission pipelines with different burial depths are shown in Figure 7- Figure11.

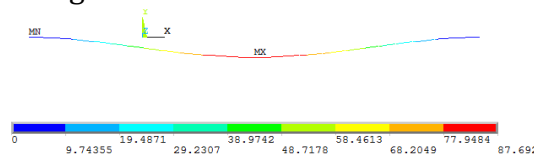


Fig.7 Deformation and displacement diagram for a burial depth of 10m

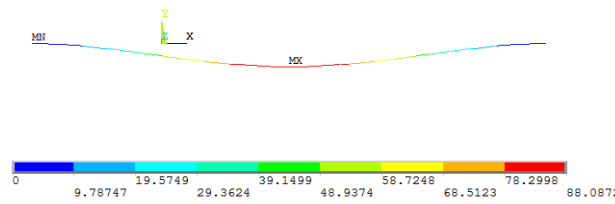


Fig.8 Deformation and displacement diagram for a burial depth of 8m

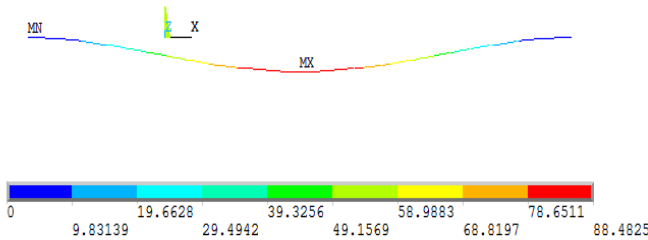


Fig.9 Deformation and displacement diagram for a burial depth of 6m

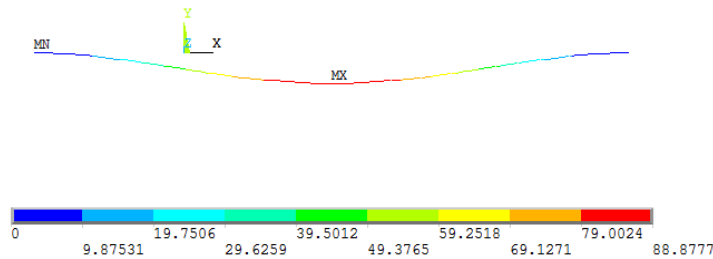


Fig.10 Deformation and displacement diagram for a burial depth of 4m

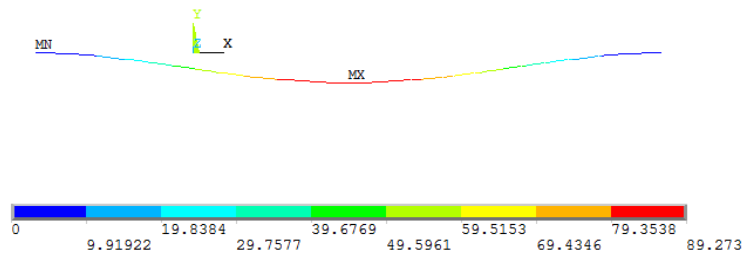


Fig.11 Deformation and displacement diagram for a burial depth of 2m

The values of bending stress and axial stress extracted from the model displacement variation for five different burial depths are shown in Table 2.

Table 2 The value of displacement, bending stress and axial stress when the pipe diameter changes

Depth of burial/m	Deformation displacement/mm	Axial stress/MPa	Y-side bending stress /MPa	Y-side bending stress /MPa
10	87.692	0.117	0.066	0.075
8	88.087	0.082	0.057	0.090
6	88.483	0.064	0.062	0.097
4	88.878	0.072	0.051	0.059
2	89.273	0.064	0.049	0.082

The values of maximum stress, relative permeability, absolute permeability, and magnetic field strength for the five different tube diameter models are shown in Table 3.

Table 3 Values of maximum stress, relative magnetic permeability, absolute magnetic permeability, and magnetic field strength when the tube diameter varies

Pipe outside diameter /mm	Maximum stress /MPa	Relative magnetic permeability	Absolute magnetic permeabilityH/m	Magnetic field strengthA/m
600	0.60	828852	1.04	4.24×10^{-5}
700	0.44	1130434	1.41	3.13×10^{-5}
800	0.21	2375905	2.98	1.48×10^{-5}
900	0.18	2764008	3.47	1.27×10^{-5}
1000	0.15	3339174	4.19	1.05×10^{-5}

The displacement variation and magnetic field strength comparison line graphs for five different pipe diameters of oil and gas transmission pipelines are shown in Figure 12 and Figure 4.13

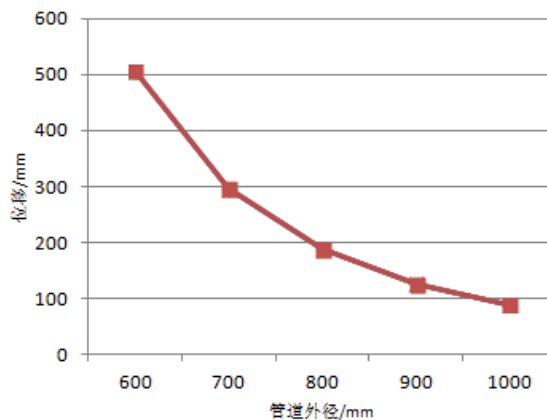


Fig.12 Variation of displacement of overhanging pipe section with pipe diameter

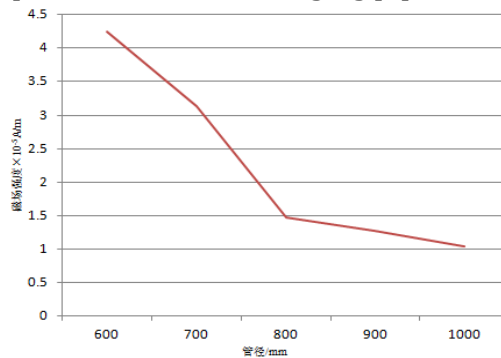


Fig.13 Variation of magnetic field strength with pipe diameter for suspended pipe section

6. Summary

By analyzing the structure and mechanics of buried oil and gas transmission pipeline, the finite element model is established and the simulation model is obtained. Analysis of the

displacement and stress distribution of the overhanging pipe section can be concluded that the displacement of the overhanging pipe section decreases nonlinearly with the increase of the pipe diameter, and the displacement changes faster when the pipe diameter is smaller. The speed of change is the fastest between 600mm and 700mm. As the diameter of the tube gradually increases, the stress gradually decreases, the relative permeability increases, and the magnetic field strength decreases, and the rate of decrease is the fastest between 600mm and 800mm, and the rate of decrease becomes slow between 800mm and 1000mm. It is presumed that the magnetic permeability increases gradually with the increase of the tube diameter. When the geomagnetic field is a certain value, the magnetic signal of the geomagnetic field will change when it passes through the suspended pipe section, and the magnetic field strength decreases with the increase of the pipe diameter.

With the increase of burial depth, the displacement variation of the suspended pipe section is close to a linear decrease. With the increase of burial depth, the stress of the unit gradually increases. The magnetic field strength gradually increases with the increase of burial depth, and the fluctuation range of magnetic field strength is smaller than that of the change of magnetic field strength affected by the pipe diameter. However, when the magnetic field strength increases, the stress obtained may be small due to problems such as grid division, so the magnetic field strength at this point is small when the burial depth is 4m. Therefore, when the magnetic field is a certain value, the magnetic signal of the geomagnetic field will change when passing through the suspended pipe section, and the magnetic field strength increases with the increase of the burial depth.

References

- [1] Dubov A.A. Study of Metal Properties Using Metal Magnetic Memory Method[A].7th European Conference on Non-destructive Testing[C]. Copenhagen,1997, (10): 920-927.
- [2] Maciej Roskosz. Metal magnetic memory testing of welded joints of ferritic and austenitic steels[J]. NDT and E International,2011,44(3).
- [3] Mahdi Moonesan,Mehrdad Kashefi. Effect of sample initial magnetic field on the metal magnetic memory NDT result[J]. Journal of Magnetism and Magnetic Materials,2018,460.
- [4] J Kaleta,P Wiewiorski.magnetovision as a tool for investigation of fatigue process of ferromagnetics[C]//SAE Brasil International Conference on Fatigue.Brasil:[s.n],2002.
- [5] Wilson J W, Gui Y T, Barrans S. Residual magnetic field sensing for stress measurement[J]. Sensors & Actuators A Physical, 2007, 135(2):381-387.
- [6] Kosoń-Schab A,Smoczek J,SzpytkoJ.CRANE FRAME INSPECTION USING METAL MAGNETIC MEMORY METHOD[J]. Journal of Kones, 2016, 23(2):185-192.
- [7] Zhong Weichang. The theoretical basis of metal magnetic memory method diagnosis-the elasto-plastic strain magnetization of ferromagnetic materials[J]. Nondestructive Testing, 2001(10): 424-426.
- [8] Gao Yatian. Research progress of metal magnetic memory detection technology for oil and gas pipelines[J]. Chemical Machinery, 2019,46(02):107-111.
- [9] Yin Dawei, Xu Binshi, Dong Shiyun, Dong Lihong, Feng Chen. Research on the changes of magnetic memory signal under different detection environments [J]. Acta Armamentarii, 2007(03): 319-323.
- [10] Li Lianxiu. Research on Magnetostriction and Magnetic Memory[J]. Nondestructive Testing, 2004(03):109-112.
- [11] Li Luming, Wang Xiaofeng, Huang Songling. The relationship between magnetic memory and geomagnetic field[J]. Nondestructive Testing, 2003(08):387-389+406.
- [12] Xu Minqiang, Li Jianwei, Leng Jiancheng, Xu Mingxiu. Mechanism model of metal magnetic memory detection technology [J]. Journal of Harbin Institute of Technology, 2010, 42(01): 16-19.